Supplementary Information (SI) for Journal of Materials Chemistry C.

Supporting Information

Natural Binder for Synchronous Management of Iodine Species Adsorption and Redox toward Sustainable Carbon-Based Perovskite Solar Cells

Experimental Section

Materials

Dimethyl-formamide (DMF, 99%), dimethyl sulfoxide (DMSO, 99.9%), isopropyl alcohol (IPA,99.9%) and ethyl acetate (EA, 99.8%) were purchased from Sigma-Aldrich, thioglycolic acid (TGA, 98%), $SnCl_2 \cdot 2H_2O$ (>99.995%) was purchased by Sigma-Aldrich. Lead iodide (PbI_2, 99%) and Methylammonium iodide (MAI, 99.5%) was purchased from Xi'an yuri solar co, Ltd. Chitosan (CTS 99.8%) and acacia gum (AG 99.8%)) were purchased from Aladdin. The commercial carbon paste (DD-10) was purchased from Guangzhou Saidi Technology Development Co, Ltd. All chemicals were used as received without further purification.

Preparation of Perovskite Precursor Solution

The $MAPbI_3$ perovskite precursor solution with a concentration of 1.8M was obtained by dissolving 143 mg MAI and 415 mg PbI_2 into 500 μL DMSO/DMF mixed solvent (V: V = 1:9), and then stirred for 4 h at 60 °C, the solution was filtered through a 0.45 μm syringe filter before use.

Device Fabrication

Glass/FTO substrates were cleaned with deionized water, acetone, and isopropyl alcohol in an ultrasonic bath for 30 min, respectively, and then dried by flowing nitrogen gas. Before use, the substrates were pretreated with O_2 plasma for 20 min. The SnO_2 electron transport layer was prepared by chemical water bath deposition, and 2.5 g urea, 2.5 mL HCl, 50 μL TGA and 0.548 g $SnCl_2 \cdot 2H_2O$ were added into 200 mL deionized water to prepare CBD mother liquor. FTO conductive glass and CBD solution were put into a glass reaction container, sealed and reacted at 90 ℃ for 5 h. After the reaction was completed, the FTO substrate deposited with SnO_2 was removed from the reaction vessel, washed ultrasonic with DI water and IPA for 5 min respectively, and the FTO was placed face-up on a hot platform at 150 ℃ for 1 h to form a dense SnO_2 electron transport layer. The SnO_2-coated substrate was treated with UVO for 20 minutes. For modified ETL, 0.05 mg/mL CTS dissolved in water solution were spin-coated on SnO_2 for 30 s at 5000 rpm, and the modified SnO_2 films were subsequently annealed for 10 min at 100 °C. The $MAPbI_3$ precursor solutions without or with AG were spin-coated onto the SnO_2 for 30 s at 4000 rpm. At the 10 s, 300 μL EA was quickly dripped on the spinning substrates, and the samples were annealed at 130 °C for 10 min. Finally, the commercial carbon paste was doctor-bladed onto the perovskite film and heated at 120 ℃ for 10 min to complete the solar cell fabrication. The above processes are all completed in air with a humidity of around 35%.

Material characterization

A field-emission scanning electron microscope (SEM, Hitachi SU8220) was used to examine the film's surface and cross-section morphologies. A powder X-ray diffraction (XRD) system (Smartlab3 KW) equipped with Cu Kα radiation was used to measure the crystal structure. The GIXRD measurement was carried out by Micromax-007HF equipment. Fourier transform infrared (FTIR) spectra were measured using an FTIR spectrometer with a NICOLET IS 50 FTIR (Thermo Fisher Scientific). X-ray photoelectron spectrometer (XPS) measurements were conducted on an ESCALAB 250XI+ system (Thermo Fisher Scientific). A Shimadzu UV2600 spectrophotometer was used to analyze the light absorption of the perovskite layer at room temperature. Ultraviolet photoemission spectroscopy (UPS) was performed by X-ray photoelectron spectrometer (ThermoFisher Nexsa). The steady-state Photoluminescence (PL) spectra were acquired using an Edinburgh FLS1000 fluorescence spectrometer excited by a 405 nm xenon lamp flame at room temperature. A picosecond pulse semiconductor exciter with a wavelength of 405 nm was utilized as the excitation source for the time-resolved photoluminescence decay (TRPL) spectrum test, and the signal was received by a PMT1700 detector.

Device characterization

J-V characteristics were measured using a Keithley 2400 digital sourcemeter and a solar simulator (Zolix SS150) under standard simulated AM 1.5 illumination (100 mW cm^{-2}). The *J–V* curves were measured with a scanning rate of voltage interval of 100 mV and delay time of 1000 ms from 1.5 to -0.1 V (reverse) or from -0.1 to 1.5 V (forward). Cells were covered by a black metal mask with an active area of 0.04 cm^2. The external quantum efficiency (EQE) of the device was obtained by the EQE measurement system (Enli Tech). Electrical impedance spectroscopy (EIS) measurements of the solar cell devices were obtained in the dark at 0.9 V bias using a CHI660E electrochemical workstation (CHI Instruments Inc.) within the frequency range of 10^{-1}–10^6 Hz.

Computational details: Calculate electrostatic surface potential and binding energy using DMol3 code in Materials Studio.

Time-resolved photoluminescence (TRPL) Measurement: Fitting parameters of the bi-exponential decay function in TRPL spectra of the corresponding perovskite films deposited on the glass substrate using a 405 nm excitation light source. The results are fitted with the bi-exponential decay Eq. (S1):

$$R(t) = A_1\exp(-t/\tau_1) + A_2\exp(-t/\tau_2) \tag{S1}$$

and the τ_{ave} is calculated by Eq. (S2):

$$\tau_{\mathrm{ave}}=(A_1\tau_1^2+A_2\tau_2^2)/A_l\tau_1+A_2\tau_2 \tag{S2}$$

$$\tau_{\mathrm{ave}}=(A_1\tau_1^2+A_2\tau_2^2)/A_l\tau_1+A_2\tau_2$$

where A_1 and A_2 represent the corresponding decay amplitudes, while τ_1 and τ_2 represent the decay time constants.

Trap Density Measurement: Calculated results of defect density (N_t) of the pristine and AS-modified devices from the *J-V* curves of SCLC measurements are shown in Figure 4c. The N_t is calculated by Eq. (S3):

$$N_{(t)} = \frac{2\varepsilon_r\varepsilon_0 V_{TFL}}{qL^2}$$

$$N_{(t)} = \frac{2\varepsilon_r\varepsilon_0 V_{TFL}}{qL^2} \tag{S3}$$

where ε_r is the relative dielectric constant, ε_0 is the vacuum permittivity, V_{TFL} is the trap-filled limit voltage, q is the elementary charge, and L is the thickness of the perovskite layer.

The light intensity dependences of V_{OC}: The ideal factor n value is calculated by Eq. (S4):

$$qV_{OC} = E_g - nkT\ln(\frac{I_0}{I}) \tag{S4}$$

Where q is the charge constant, V_{OC} is the open circuit voltage, E_g is the bandgap width, k is the Boltzmann constant, T is the temperature during testing, I_0 is the incident light intensity, and I is the absorbed light intensity.

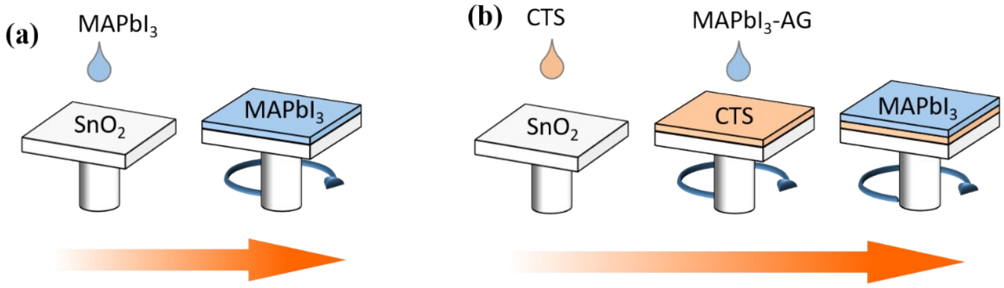

Fig. S1. Schematic illustration of the preparation process for the pristine and modified films.

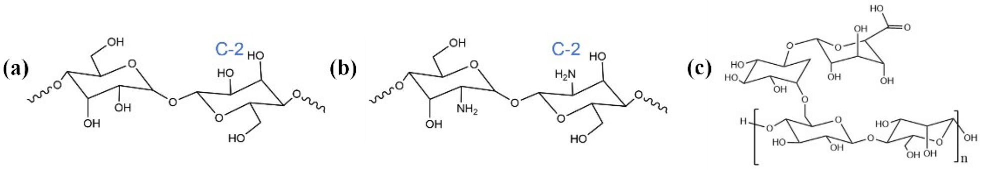

Fig. S2. (a, b, c) Molecular structural formulas of amylose, chitosan and acacia gum.

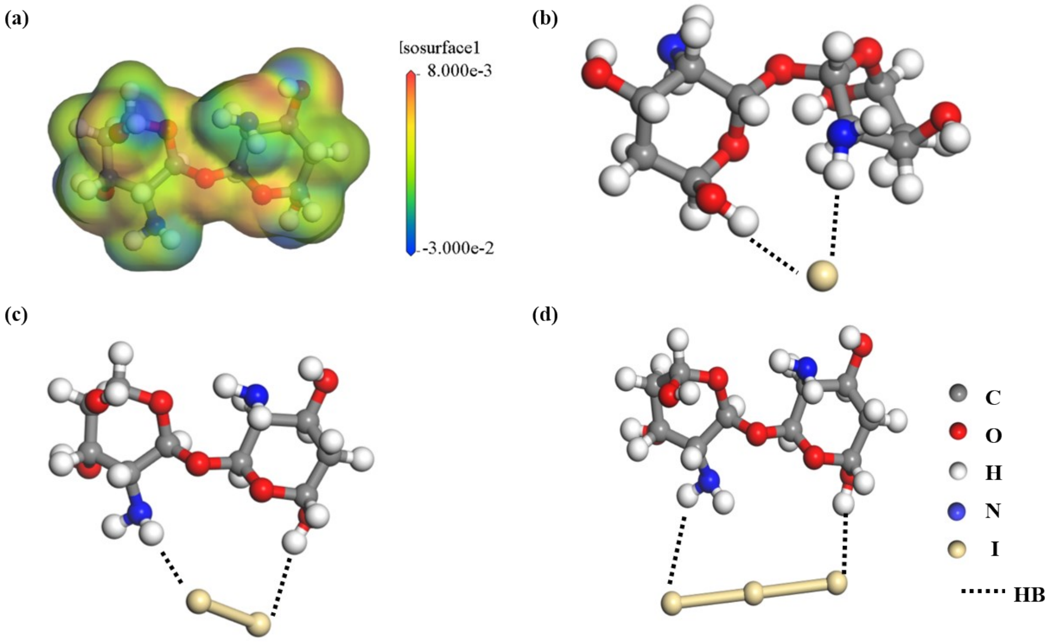

Fig. S3. (a) ESP of the CTS. (b, c, d) The optimized structure of CTS combined with I^- and I^0, I_3^-.

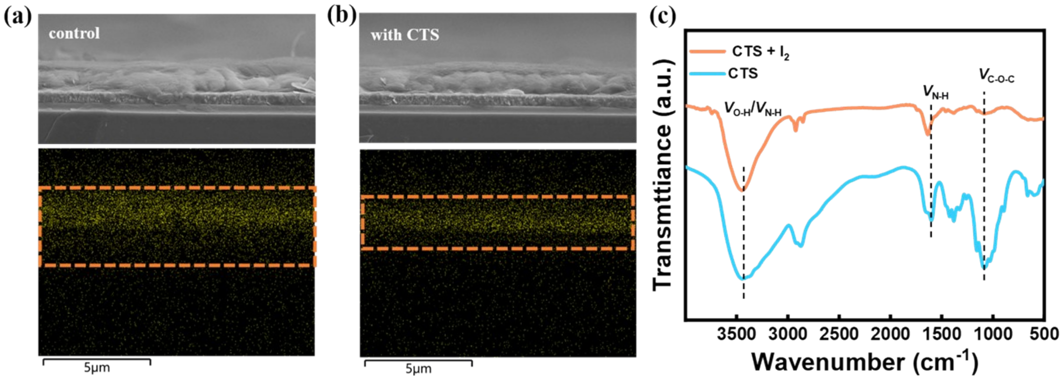

Fig. S4. (a,b) Cross-sectional SEM and EDS of iodine, control and modified CTS devices after aging time. (c) FTIR spectra in the wavenumber range between 500 and 4,000 cm^{-1} of CTS mixed with I_2 and pure CTS.

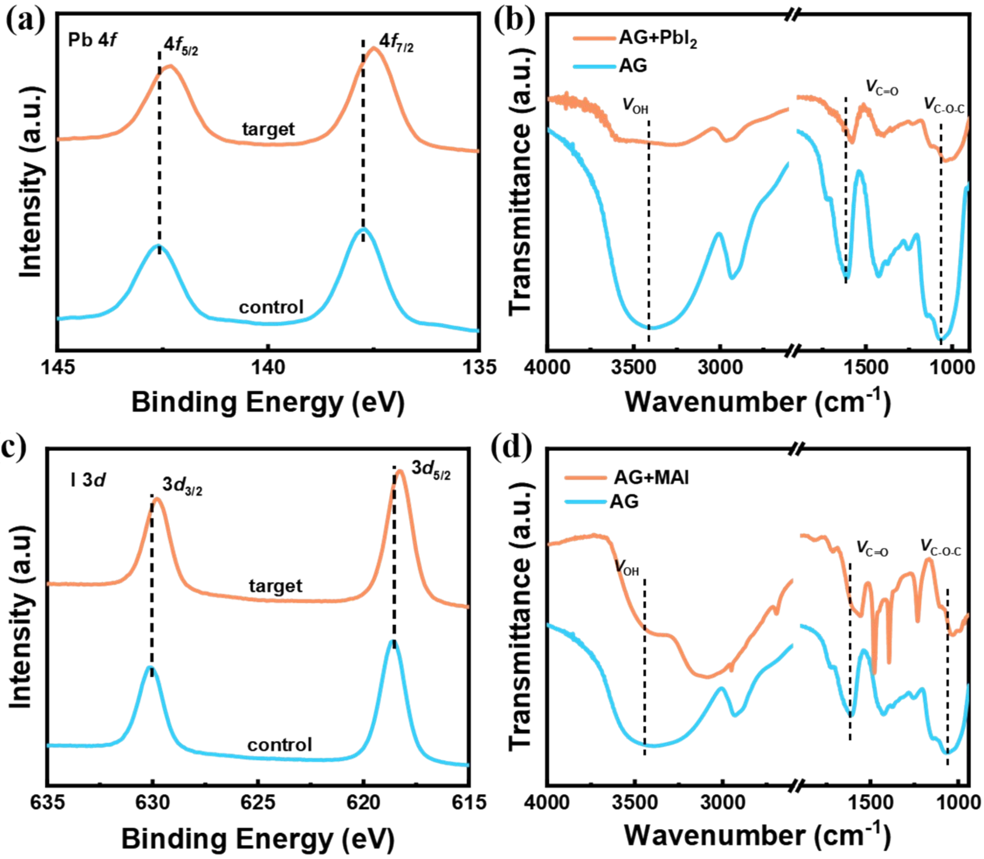

Fig. S5. (a) Pb 4f XPS spectra of the perovskite film and AG-modified perovskite films. (b) FTIR spectra in the wavenumber range between 900 and 4,000 cm^{-1} of PbI_2 mixed with AG and pure AG. (c) I 3d XPS spectra of the pristine and AG-modified perovskite films. (d) FTIR spectra in the wavenumber range between 900 and 4,000 cm^{-1} of MAI mixed with AG and pure AG.

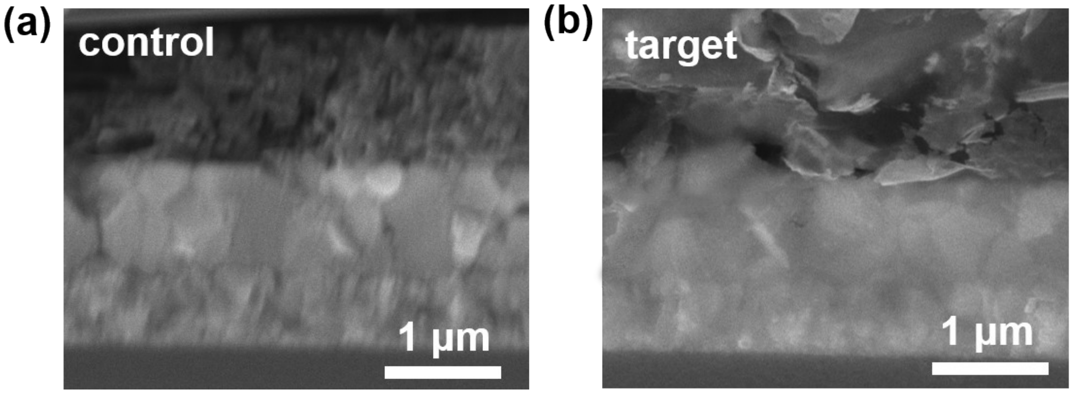

Fig. S6. (a) Cross-sectional SEM images of (a) the pristine perovskite film and (b) perovskite with AG film.

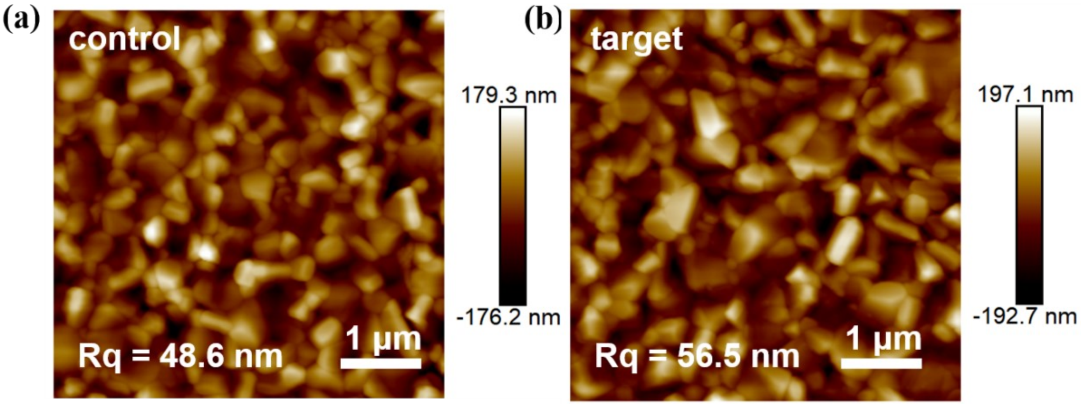

Fig. S7. (a) AFM images of the perovskite films without and (b) with AG modification.

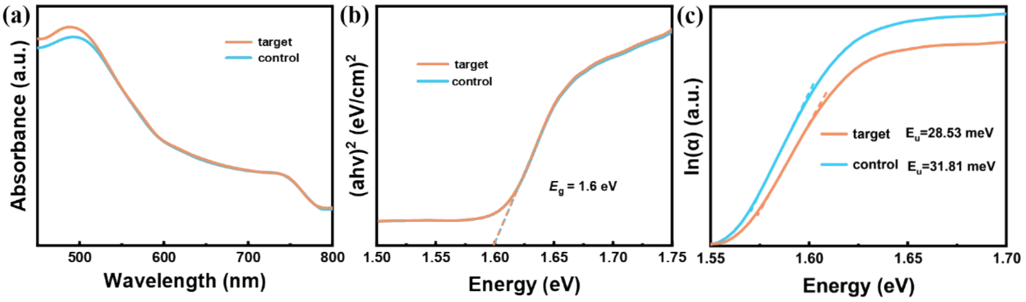

Fig. S8. (a) UV-vis absorption spectra of the pristine and AG-modified perovskite films (b) the corresponding Tauc plot of the pristine and AG-modified perovskite films (c) logarithm of absorption coefficient α versus photon energy of the pristine and AG-modified perovskite films.

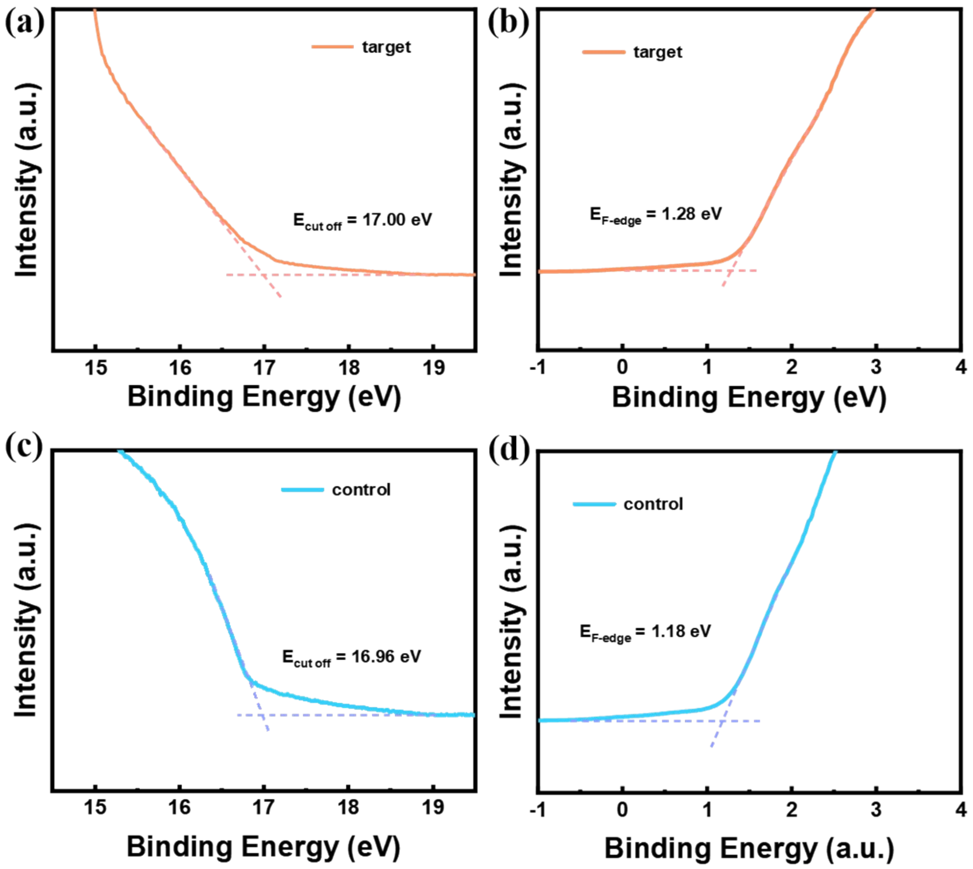

Fig. S9. (a, c) Cut-off energy ($E_{cut\ off}$), and (b, d) femi edge ($E_{F\text{-}edge}$) of the perovskite films without and with AG.

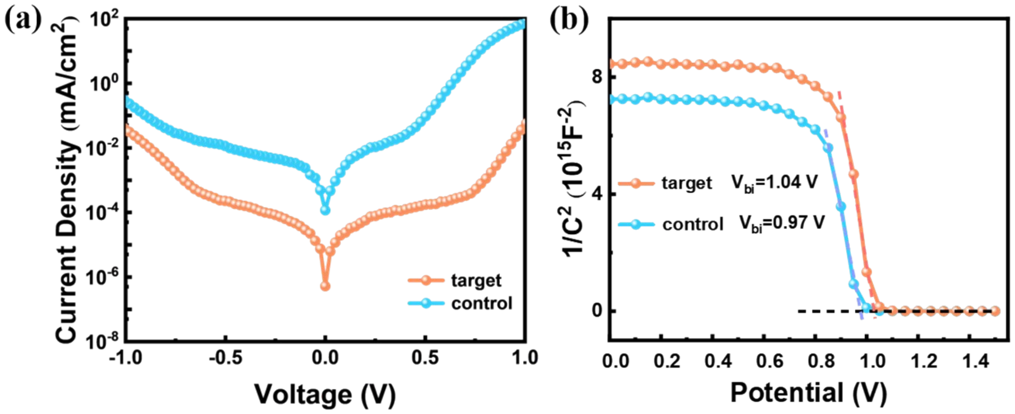

Fig. S10. (a) Curve of dark *J-V* for the pristine and AG-modified devices. (b) Mott–Schottky of the pristine and AG-modified devices.

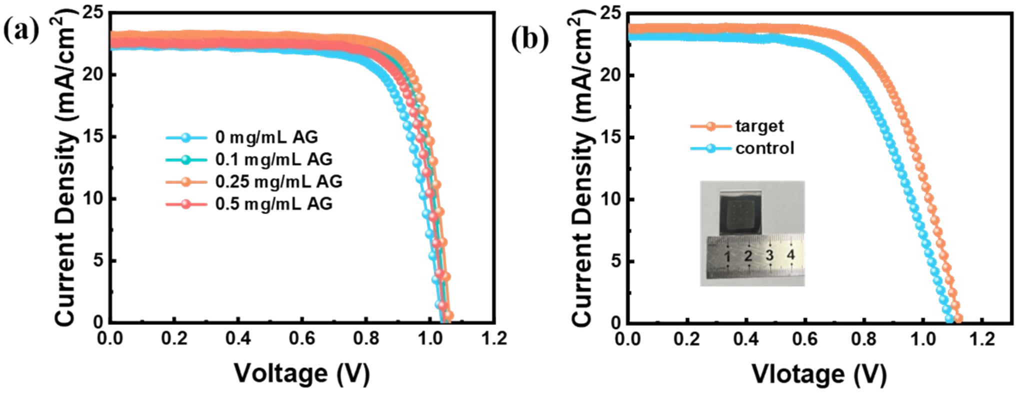

Fig. S11. (a) *J*–*V* curves of the pristine and optimum concentration of AG devices. (b) *J*–*V* curves of the pristine and CTS and AG synchronously modified devices.

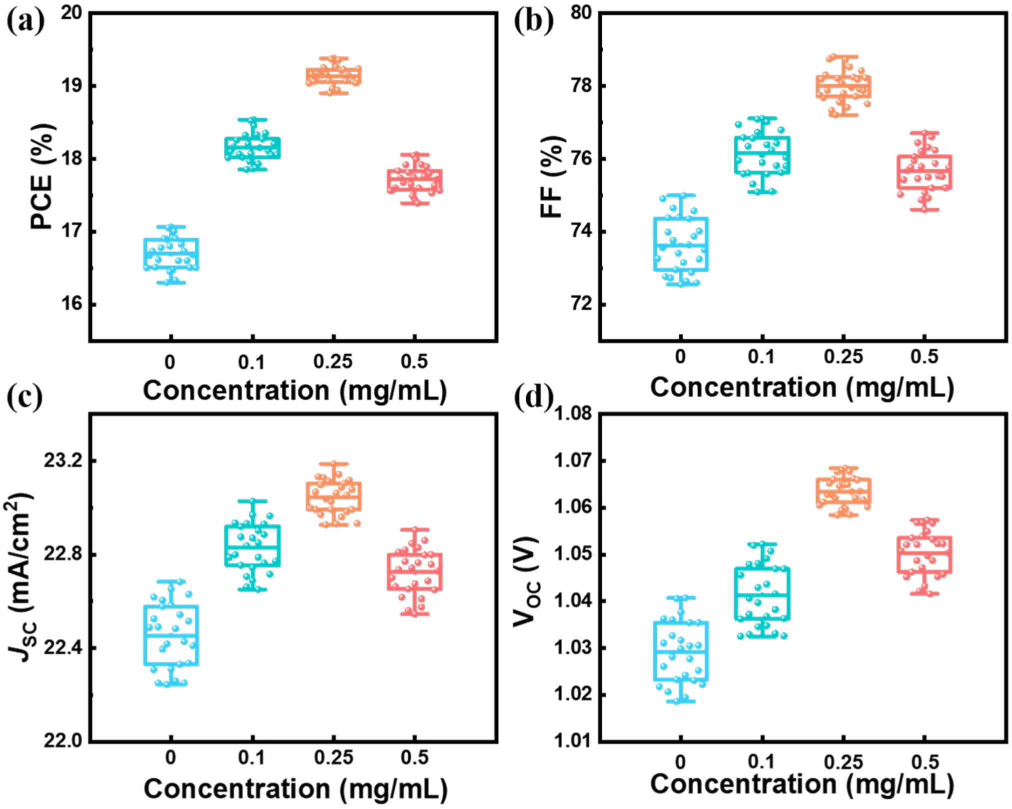

Fig. S12. (a) PCE, (b) FF, (c) J_{SC}, and (d) V_{OC} photovoltaic parameters for the PSCs modified by different AG concentrations ratios.

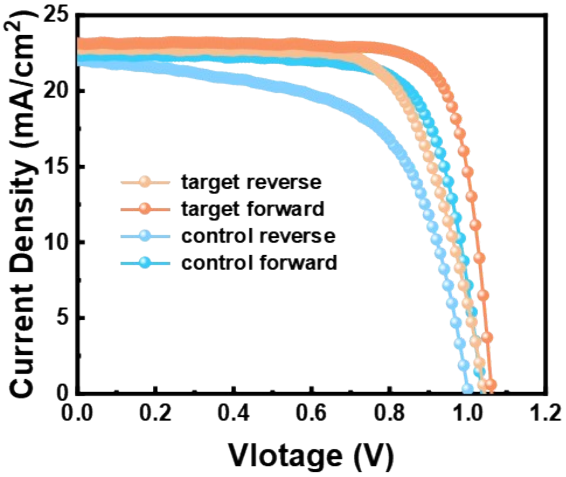

Fig. S13. The reverse and forward scans measure the best pristine and AG-modified device *J*-*V* curves.

Table S1. Fitting results of the TRPL spectra of pristine and AG-modified perovskite films.

Devices	A_1	τ_1 (ns)	A_2	τ_2 (ns)	τ_{ave} (ns)
AG-PVK	0.181	30.85	0.727	145.10	139.36
PVK	0.426	8.10	0.494	88.55	82.67

Table S2. Parameters of trap-state density of pristine and AG-modified PSCs.

Devices	V_{TFL}	L (nm)	ε_r	ε_0(F cm $^{-1}$)	N_t (cm $^{-3}$)
control	0.51	850	28.8	8.85×10^{-14}	2.25×10^{15}
target	0.32	850	28.8	8.85×10^{-14}	1.41×10^{15}

Table S3. Fitting results of the Nyquist plots of pristine and AG-modified PSCs.

Devices	R_s (Ω)	R_{rec} (Ω)
SnO_2	141.1	19,766
SnO_2/AS	116.9	26,362

Table S4. Photovoltaic parameters of champion PSCs of pristine and AG-modified scanned from forward and reverse directions.

Devices	Scan Direction	J_{SC} (mA cm $^{-2}$)	V_{OC} (V)	FF (%)	PCE (%)
control	Reverse	22.34	1.037	73.57	17.04
	Forward	22.04	1.002	61.41	13.56
target	Reverse	23.15	1.066	78.58	19.38
	Forward	22.82	1.044	69.53	16.57

Table S5. Summary of the champion and average photovoltaic parameters of the devices modified by different concentrations of AG.

Devices		J_{SC} **(mA/cm^2)**	V_{OC} **(V)**	**FF（%）**	**PCE (%)**
0 mg/mL	Average	22.45 ± 0.23	1.029 ± 0.011	73.63 ± 1.36	16.69± 0.36
	Champion	22.34	1.037	73.57	17.04
0.1 mg/mL	Average	22.83± 0.20	1.044 ± 0.008	76.14 ± 0.96	18.28 ± 0.27
	Champion	22.91	1.051	77.00	18.54
0.25 mg/mL	Average	23.05± 0.15	1.063 ± 0.005	77.85± 0.78	19.13 ± 0.23
	Champion	23.14	1.066	78.58	19.38
0.5 mg/mL	Average	22.75 ± 0.19	1.050 ± 0.007	75.70 ± 1.06	17.75± 0.32
	Champion	22.60	1.045	76.50	18.06

Table S6. Summary of the champion and average photovoltaic parameters of the devices modified by different concentrations of CTS.

Devices		J_{SC} **(mA/cm^2)**	V_{OC} **(V)**	**FF（%）**	**PCE (%)**
0 mg/mL	Average	22.45 ± 0.23	1.029 ± 0.011	73.63 ± 1.36	16.69± 0.36
	Champion	22.34	1.037	73.57	17.04
0.025 mg/mL	Average	22.56± 0.25	1.054 ± 0.008	75.77 ± 1.22	18.01 ± 0.33
	Champion	22.67	1.062	76.19	18.35
0.05 mg/mL	Average	22.87±0.17	1.059±0.012	77.23±1.19	18.92±0.28
	Champion	22.92	1.072	78.17	19.21
0.1 mg/mL	Average	22.75 ± 0.21	1.057 ± 0.011	76.84 ± 1.25	18.53± 0.30
	Champion	22.86	1.069	77.05	18.82

Table S7. The champion values of photovoltaic parameters of perovskite solar cells of the control, AG, CTS, CTS and AG synchronously modified devices.

Devices		J_{SC} **(mA/cm^2)**	V_{OC} **(V)**	**FF（%）**	**PCE (%)**
control	Average	22.45 ± 0.23	1.029 ± 0.011	73.63 ± 1.36	16.69± 0.36
	Champion	22.34	1.037	73.57	17.04
CTS	Average	22.87±0.17	1.059±0.012	77.23±1.19	18.92±0.28
	Champion	22.92	1.072	78.17	19.21
AG	Average	23.05± 0.15	1.063 ± 0.005	77.85± 0.78	19.13 ± 0.23
	Champion	23.14	1.066	78.58	19.38
CTS and AG	Average	23.00 ± 0.16	1.076 ± 0.004	78.16± 0.60	19.37± 0.17
	Champion	23.08	1.08	78.50	19.53